Published in final edited form as:
J Surg Res. 2012 August ; 176(2): 359–366. doi:10.1016/j.jss.2011.10.025.

Novel Immunocompetent Murine Models Representing Advanced Local and Metastatic Pancreatic Cancer

Elizabeth Little, **Cindy Wang**, **Patricia Watson**, **Dennis Watson**, **David Cole**, and **Ramsay Camp**

Abstract

Background—The development of novel therapeutics for pancreatic cancer has been hindered by a lack of relevant preclinical models. The purpose of this study was to evaluate the clinical relevancy of two pancreatic cancer models using standard-of-care therapeutic agent gemcitabine.

Materials and Methods—Murine Panc02 cells were injected directly into the spleen or pancreas of C57Bl/6 mice to respectively create models of metastatic and locally advanced pancreatic cancer. Beginning 7 days post-Panc02 injection, treated mice received 20mg/kg gemcitabine i.p. every three days. Animals were sacrificed when the untreated mice became moribund and tumor/liver weight used to assess tumor burden.

Results—Untreated mice became moribund 22 days after pancreatic Panc02 injection. Gross analysis revealed localized pancreatic tumors weighing 1.063g. Intrasplenic Panc02 injection produced extensive liver metastasis by day 15 when the untreated mice first became moribund. Liver weights at this time averaged 3.6g compared to the average non-tumor-bearing weight of 1.23g. Gemcitabine therapy resulted in a 54% decrease in localized pancreatic tumor weight and 62.5% decrease in metastatic liver weight. Additionally, gemcitabine therapy extended animal survival to 20.5 days compared to 18.0 day average for the untreated mice.

Conclusions—We describe two models depicting both locally advanced and metastatic pancreatic cancer in immunocompetent mice. In efforts to establish baseline therapeutic efficacy, we determined that gemcitabine reduces tumor burden in both models and enhances survival in the metastatic model. These clinically relevant models provide valuable tools to evaluate novel therapeutics in pancreatic cancer.

Introduction

With nearly 37,000 estimated deaths in 2010, pancreatic adenocarcinoma is the fourth leading cause of cancer-related deaths in the United States. While surgery is the only curative option, fewer than 20% of patients are eligible for surgery due to the metastatic spread at the time of diagnosis [1]. Besides surgery, treatment with the chemotherapeutic agent gemcitabine is typically regarded as standard of care in efforts to extend survival and to provide palliative care [1–2]. In initial Phase III clinical trials, gemcitabine prolonged survival only about 6 months, nearly 2 months longer than 5-Fluorouracil [3–4] and extended 1 year-survival to 18% compared to 2% in the 5-FU arm [4]. The exceedingly poor prognosis for patients with pancreatic cancer necessitates further development of novel therapeutic approaches.

A major challenge in the development of novel pancreatic cancer therapies is the lack of appropriate preclinical animal models. *In vivo* investigations of pancreatic cancer most often employ xenograft implants. This method, using either subcutaneous or orthotopic injections, is typically performed in immunocompromised mice, creating an artificial tumor environment and ignoring the effect of the host immune system on tumor development [5]. Other animal models include carcinogen-induced models, which produce an accurate

recreation of carcinogenesis but may affect tissues other than the pancreas [5], and genetically engineered models, which focus on specific gene involvement in cancer development but are often not capable of imitating more advanced cancers as well as xenograft models [6]. On the other hand, genetically engineered models may be of particular interest in studying pancreatic intraepithelial neoplasia (PanIN) stages and pancreatic cancer development [7].

Panc02 cells, first described in 1984, were obtained from ductal adenocarcinoma in a C57B1/6 mouse [8] and, uniquely, allow for an immunocompetent murine model of pancreatic cancer. Several investigators, including our group, have begun to take advantage of this syngeneic system, typically by either subcutaneous [9–15] or orthotopic models [16–18]. Subcutaneous tumors offer the advantage of directly assessing tumor burden but do not metastasize as often as human pancreatic cancer or otherwise mimic human disease [19–20]. Orthotopic or metastatic models are more clinically relevant but present a different challenge in measuring tumor burden. Bioluminescence imaging (BLI) is one method of detecting and measuring tumor growth *in vivo*. By transfecting tumor cells with *Photinus pyralis* luciferase gene, these cells emit light at 560nm in the presence of ATP and D-luciferin substrate and photons can be measured using charge coupled device cameras. This light emission has been shown useful in identifying and quantifying tumor growth in individual rodents over time in both subcutaneous and orthotopic models [21–23].

Here, we present two clinically relevant immunocompetent animal models of pancreatic cancer, representing the continuum of pancreatic cancer from a localized tumor in the pancreas to widespread liver metastasis from portovenous infiltration. Our complimentary models allow evaluation of novel therapeutic strategies at various stages of cancer development. Furthermore, we demonstrate baseline drug efficacy in our models by treatment with gemcitabine, serving as a foundation to build novel future combination strategies.

Methods

Cells

Murine Panc02 cells were obtained from the NCI DCTD Tumor Repository (NCI, Frederick, MD). Panc02 cells were stably transfected based on G418 antibiotic selection (1mg/mL in media) with a *Photinus pyralis* luciferase gene to be used for bioluminescent imaging Panc02-luc cells were maintained in RPMI 1640 media supplemented with 2mM L-glutamine (Hyclone, Logan, TX), 200ug/mL G418 (Invitrogen, Carlsbad, CA), and 10% fetal bovine serum (Hyclone) at 37°C in 5% CO_2.

Animals

8–12 week old C57B1/6 mice were used for these experiments, which were performed according to protocols approved by the Institutional Animal Care and Use Committee at the Medical University of South Carolina. Animals were bred and housed in a pathogen-free, biohazard barrier facility. Mice were euthanized by CO_2 asphyxiation followed by cervical dislocation.

Tumor Cell Injections

Mice were anesthetized using 0.2ml/10gm body weight of 1.2% Avertin (2,2,2-Tribromoethanol; Sigma Aldrich, St. Louis, MO) solution i.p. and received a single, preemptive analgesic of 3mg/kg carprofen (Sigma Aldrich). The left flank was shaved and sterilized with Betadine (Purdue Products, Stamford, CT). Once surgical plane anesthesia was achieved, 1 cm left subcostal incision was made through the abdomen skin and

peritoneum. For the localized pancreas model, 1×10^6 Panc02-luc cells in 0.05mL PBS (Hyclone) were injected into the exteriorized pancreas using a sterile 28-gauge needle and hypodermic syringe. For the intrasplenic injections in the metastatic model, 1×10^6 Panc02-luc cells in 0.1mL PBS (Hyclone) were injected directly into the tip of the exteriorized spleen using a 28-gauge needle and hypodermic syringe. Animals were sacrificed if evidence of pain or suffering was present.

Gemcitabine Therapy

Mice were treated with 20mg/kg i.p. of gemcitabine every three days, beginning 7 days after Panc02-luc injection. Gemcitabine therapy continued until the untreated mice became moribund, which occurred at day 15 in the intrasplenic model and at day 22 in the pancreatic model. Animals were monitored daily for health, and moribundity was determined by a blinded investigator.

Bioluminescence Imaging (BLI)

Mice were anesthetized in an induction chamber with 5% isoflurane (Novaplus, Irving, TX). Each mouse received an i.p. injection of 3mg D-luciferin (Invitrogen) in 200uL PBS. The mice were then placed in the heated chamber of the Xenogen optical imaging device with nose cones to deliver 1.5% isoflurane. Up to five mice were imaged at a time until peak luminescence. Mice were then removed from the instrument, sacrificed by cervical dislocation, and organs (liver, spleen, and pancreas) harvested for *ex vivo* imaging.

Histological Analysis

Following sacrifice, tumors were resected, fixed overnight in 10% buffered formalin, set in paraffin blocks, and cut into 5um thick sections. Sections were stained with standard hematoxylin and eosin staining. Terminal deoxynucleotidyl transferase dUTP nick end labeling (TUNEL) was performed according to manufacturer's directions using the DeadEnd Colorimetric TUNEL System (Promega, Madison, WI). TUNEL-positive cells were quantified at 20x (localized model) and 40x (metastatic model) magnification, with at least three random fields counted per section. Antigen retrieval was performed prior to Ki67 staining by immersing the slides in 10mM citrate buffer (pH 6.0, Antigen Unmasking Solution; Vector Labs, Burlingame, CA) and microwaving for 10 minutes. Sections were stained with anti-Ki67 antibody (Abcam #15580, Cambridge, MA) overnight at 1:750 dilution. Secondary antibody and DAB chromogen detection was performed following the manufacturer's protocol (Rabbit IgG Vectastain Elite ABC kit, Vector Labs). Ki-67 positive cells were counted at 40x magnification, with at least three random fields counted per section. Ki-67 and TUNEL staining from hepatic tumors of the metastatic model were also quantified at the tumor-border interface, with three fields counted per section at 20x magnification.

Statistical Analysis

Statistical analysis was performed using GraphPad Prism 5 software (La Jolla, CA). Kaplan Meier survival analysis was used for the metastatic moribundity study. Linear regression analysis was used to identify correlations between bioluminescence total flux and tumor weight, with a p-value less than 0.05 considered significant for identifying the existence of a relationship and a Goodness-of-Fit R^2 value to determine the extent of said relationship. Two-tailed unpaired students' t-tests were used for statistical analysis in all other experiments, with a *P*-value less than 0.05 considered significant.

Results

Intrasplenic and pancreatic Panc02 injections result in consistent tumor growth

Pancreatic injections produced localized pancreatic tumors with no metastasis grossly observed (Figure 1a). The first untreated mice became moribund 22 days after Panc02 injection. Upon sacrifice at this timepoint, the average tumor in the untreated group had a volume of 1276 ± 354.2 mm^3. Intrasplenic injection generated a spleen tumor at the injection site as well as extensive metastasis throughout the liver (Figure 1b). As this model results in hepatic metastasis too extensive to isolate, liver weight was used to quantify tumor burden. Untreated mice become moribund at an average of 18 days post-tumor injection and the average liver weighs 3.6 ± 0.22g at the time of sacrifice compared to the average non-tumor-bearing liver weight of 1.23 ± 0.065g (P=0.001, data not shown). H&E sections confirm tumor presence in both the localized pancreatic (Figure 1a) and the metastatic (Figure 1b) models.

Gemcitabine decreases tumor burden in localized and metastatic models

As gemcitabine remains the focus of chemotherapy regiments for locally advanced and metastatic pancreatic cancer, we aimed to assess its effect in both *in vivo* models establishing a therapeutic baseline to assess novel combination therapies. Gemcitabine therapy resulted in a 54% decrease in tumor weight in the localized model, with an average weight of 1.063 ± 0.22g in the untreated mice and 0.5756 ± 0.07g in the gemcitabine treated mice (Figure 2a, P=0.028). Tumor volume also decreased with chemotherapy, resulting in a 36% decrease from an average 1276 ± 354.2mm^3 in the untreated group compared to 458.7 ± 57.88mm^3 (Figure 2b, P=0.0152). Similar treatment effect was observed in the metastatic model. Fifteen days post-tumor cell injection, the average gemcitabine treated liver weighed 2.25 ± 0.46g compared to the untreated average of 3.6 ± 0.22g, corresponding to a 62.5% decrease in tumor burden (Figure 2c, P=0.02).

Gemcitabine enhances animal survival in the metastatic model

In a parallel study, we evaluated the effect of gemcitabine in animal moribundity using the intrasplenic metastatic model. Gemcitabine therapy was continued until 16 days post-tumor injection, when the untreated mice first became moribund. Animal health was assessed daily by a blinded investigator and mice were sacrificed as they became moribund. Gemcitabine therapy significantly increased survival to an average of 20.5 days from the untreated average of 18.0 days (Figure 2d, P=0.004).

Gemcitabine decreases proliferation in the localized tumor model

Mechanistically, gemcitabine is a deoxycytidine analogue that is metabolized into two prodrugs: gemcitabine diphosphate (which inhibits ribonucleotide reductase from generating deoxyribonucleotides for DNA synthesis) and gemcitabine triphosphate (which competes with deoxycytidine 5'triphosphate for incorporation into the DNA, leading to masked chain termination) [24]. Because of this, we next investigated whether gemcitabine altered proliferation and apoptosis in either model by investigating Ki-67 and TUNEL expression in the tumor sections. Immunohistochemistry was performed on tumor sections from the untreated and gemcitabine-treated mice sacrificed 15 days (metastatic model) and 22 days (localized model) after Panc02 injection. While gemcitabine therapy did not alter apoptosis in the localized pancreatic tumors (Figure 3a, P=0.3973), decreased proliferation was observed with reduced Ki67 expression in the gemcitabine-treated group compared to the untreated (Figure 3b, P=0.0009). Surprisingly, there were no significant differences between the treated and untreated hepatic sections by either TUNEL (Figure 4a left, P=0.4657) or Ki-67 (Figure 4a right, P=0.5328) staining when analyzing random fields in each section.

With the large tumor burden observed in the liver metastasis model, we hypothesized that the lack of effect on proliferation and apoptosis may be a result of decreased delivery to the central portions of the tumor masses. We further analyzed the effect of gemcitabine by specifically assessing the tumor-normal tissue interface where the hepatic tumors may be better vascularized and, therefore, receive better drug delivery. When analyzing the sections at the tumor interface, however, we did not observe significant differences between the treated and untreated tumors in either TUNEL (Figure 4b left, P=0.6446) or Ki-67 (Figure 4b right, P=0.8553). Further evaluation is needed to investigate the mechanistic effect of gemcitabine in both the localized and metastatic models.

Bioluminescence Imaging (BLI) does not adequately quantify tumor burden

Due to challenges monitoring and quantitating orthotopic tumor growth, we aimed to use *in vivo* BLI to longitudinally follow growth. In our metastatic gemcitabine study, mice were imaged on days 7 and 14 prior to sacrifice on day 15. Although we observed a significant decrease in liver weight (Figure 2c), there was no significant difference in bioluminescence between the two groups on either day 7 (P=0.8742) or day 14 (P=0.5053) (Figure 5a). Average bioluminescence in the gemcitabine-treated group was decreased at day 14 compared to the untreated (0.75×10^6 photons/second compared with 1.03×10^6 photons/second) but high variability made these values statistically insignificant. Furthermore, when BLI output from day 14 was compared with liver weight at day 15, there was no significant correlation (Figure 5b, P=0.1592, R^2=0.1879)

Other investigators have found that *in vivo* measurements may be complicated by the dark skin and fur of the C57/Bl6 mice as well as the depth of the organs of interest [25]. Therefore, we aimed to use *ex vivo* luminescence by imaging the organs alone to provide a quantitative measure to tumor burden, although this would eliminate the longitudinal aspect of BLI. Nine mice were injected with 1×10^6 Panc02-luc cells in each model and sacrificed 16 (splenic) and 15 (pancreatic) days post-Panc02 injection. At this time, mice underwent BLI and, once peak luminescence was obtained, animals were quickly sacrificed and tumor-bearing organs harvested for *ex vivo* imaging. For both models, *ex vivo* imaging provided higher flux (photons/second) compared to *in vivo* (data not shown). Linear regression of the intrasplenic model comparing bioluminescence to liver weight showed that, while a relationship did exist between the two measurements of tumor-burden (P=0.0407), the bioluminescence output did not adequately predict the extent of tumor-burden as measured by liver weight (R^2=0.4727) (Figure 5c). These results were even less significant in the localized pancreatic model, where no correlation was observed between bioluminescence and tumor weight (Figure 5d, P=0.3942, R^2=0.0920). Therefore, we determined that BLI is not a reliable measurement of tumor burden in our orthotopic models.

Discussion

Pancreatic cancer *in vivo* research is hampered by a lack of clinically relevant animal models. We have presented both a localized pancreatic cancer model and an advanced metastatic model of pancreatic cancer based on portal venous invasion. Treatment with pancreatic cancer standard-of-care chemotherapeutic gemcitabine was performed in order to test the clinical relevancy of the two models. As expected, both localized and metastatic tumor burden was decreased with gemcitabine therapy compared to the untreated controls (Figures 2a and 2c). In addition, gemcitabine was found to significantly enhance animal survival in the metastatic model (Figure 2d). Despite decreased tumor burden, immunohistochemistry revealed no gemcitabine-enhanced differences in either apoptosis (TUNEL) or cell proliferation (Ki-67) in the metastatic hepatic tumors (Figure 4). The localized pancreatic tumors demonstrated decreased Ki-67 expression in the gemcitabine-treated group compared to the untreated but TUNEL staining was similar between the two

groups (Figure 3). Given gemcitabine's proposed mechanism in both proliferation and apoptosis, the lack of alterations in Ki-67 and TUNEL expression is surprising. Perhaps other markers of apoptosis and proliferation would have provided results more congruent with the observed gemcitabine-enhanced reductions in tumor burden. In addition, we used a gemcitabine dosage of 20mg/kg every 3 days which is considerably lower than the weekly Human Equivalent Dosage of 1000mg/m^2 (about 332.5mg/kg for a 20g mouse). Although 20mg/kg was enough to reduce tumor size (as measured by weight and volume) and enhance survival, it is possible that the higher clinical regimen would provide better mechanistic drug understanding and would further enhance the observed chemotherapeutic benefits.

Since the tumor location in both models prevents investigators from longitudinally measuring tumor growth, we anticipated that bioluminescence imaging would provide an *in vivo* measurement over time as well as an *ex vivo* quantification of tumor burden. However, BLI resulted in high variability which did not correlate well with tumor weight (Figure 5). Therefore, neither *in vivo* nor *ex vivo* BLI provides accurate assessment of tumor burden in either of our models. Previous studies in other laboratories have found that BLI correlation decreases with increased tumor burden [26–27] though the reason for this is not quite clear. Larger tumors have increased density and mass which may decrease the transport of substrate to the tumor center [22, 26] or decrease the photon signal because of light scattering and absorption caused by increased tissue depth [27]. Other theories include decreased detection within necrotic and hypoxic tumor regions and the presence of ascites fluid which diminishes the signal [27]. Although tumor and liver weight is sufficient, alternate methods to evaluate tumor burden – especially longitudinally – would be beneficial. Future improvements (e.g., enhanced BLI producing gene vectors) may make this possible.

In summary, we have developed consistent and clinically relevant tumor models that depict both advanced localized and metastatic disease, although longitudinal analysis and quantification of tumor burden remains a hurdle in the use of these models. In human pancreatic cancer, gemcitabine provides a fundamental role as standard of care treatment as well as neoadjuvant therapy in localized disease. Both metastatic and localized murine models predictably respond to gemcitabine, proving the clinical relevancy of the models and providing a foundation for testing novel therapeutics.

References

1. Cancer Facts & Figures. Atlanta: American Cancer Society; 2010.
2. Moss RA, Lee C. Current and emerging therapies for the treatment of pancreatic cancer. Onco Targets Ther. 2010; 3:111–127. [PubMed: 20856847]
3. Ishii H, et al. Impact of gemcitabine on the treatment of metastatic pancreatic cancer. J Gastroenterol Hepatol. 2005; 20(1):62–66. [PubMed: 15610448]
4. Burris HA 3rd, et al. Improvements in survival and clinical benefit with gemcitabine as first-line therapy for patients with advanced pancreas cancer: a randomized trial. J Clin Oncol. 1997; 15(6): 2403–2413. [PubMed: 9196156]
5. Ding Y, et al. Modeling pancreatic cancer in vivo: from xenograft and carcinogen-induced systems to genetically engineered mice. Pancreas. 39(3):283–292. [PubMed: 20335777]
6. Cespedes MV, et al. Mouse models in oncogenesis and cancer therapy. Clin Transl Oncol. 2006; 8(5):318–329. [PubMed: 16760006]
7. Hruban RH, et al. Pathology of genetically engineered mouse models of pancreatic exocrine cancer: consensus report and recommendations. Cancer Res. 2006; 66(1):95–106. [PubMed: 16397221]
8. Corbett TH, et al. Induction and chemotherapeutic response of two transplantable ductal adenocarcinomas of the pancreas in C57BL/6 mice. Cancer Res. 1984; 44(2):717–726. [PubMed: 6692374]

9. Tseng WW, et al. Development of an orthotopic model of invasive pancreatic cancer in an immunocompetent murine host. Clin Cancer Res. 16(14):3684–3695. [PubMed: 20534740]
10. Maletzki C, et al. Pancreatic cancer regression by intratumoural injection of live Streptococcus pyogenes in a syngeneic mouse model. Gut. 2008; 57(4):483–491. [PubMed: 18025068]
11. Nagaraj S, et al. Dendritic cells pulsed with alpha-galactosylceramide induce anti-tumor immunity against pancreatic cancer in vivo. Int Immunol. 2006; 18(8):1279–1283. [PubMed: 16772371]
12. Zyromski NJ, et al. Obesity potentiates the growth and dissemination of pancreatic cancer. Surgery. 2009; 146(2):258–263. [PubMed: 19628082]
13. Gnerlich JL, et al. Induction of Th17 cells in the tumor microenvironment improves survival in a murine model of pancreatic cancer. J Immunol. 2010; 185(7):4063–4071. [PubMed: 20805420]
14. Kim HS, et al. Enhancement of antitumor immunity of dendritic cells pulsed with heat-treated tumor lysate in murine pancreatic cancer. Immunol Lett. 2006; 103(2):142–148. [PubMed: 16313973]
15. Clary BM, et al. Active immunotherapy of pancreatic cancer with tumor cells genetically engineered to secrete multiple cytokines. Surgery. 1996; 120(2):174–181. [PubMed: 8751580]
16. Ziske C, et al. Increase of in vivo antitumoral activity by CD40L (CD154) gene transfer into pancreatic tumor cell-dendritic cell hybrids. Pancreas. 2009; 38(7):758–765. [PubMed: 19546834]
17. Dineen SP, et al. The Adnectin CT-322 is a novel VEGF receptor 2 inhibitor that decreases tumor burden in an orthotopic mouse model of pancreatic cancer. BMC Cancer. 2008; 8:352. [PubMed: 19038046]
18. Okudaira K, et al. Blockade of B7-H1 or B7-DC induces an anti-tumor effect in a mouse pancreatic cancer model. Int J Oncol. 2009; 35(4):741–749. [PubMed: 19724910]
19. de Jong M, Maina T. Of mice and humans: are they the same?--Implications in cancer translational research. J Nucl Med. 2010; 51(4):501–504. [PubMed: 20237033]
20. Garber K. Realistic rodents? Debate grows over new mouse models of cancer. J Natl Cancer Inst. 2006; 98(17):1176–1178. [PubMed: 16954466]
21. Jenkins DE, et al. Bioluminescent imaging (BLI) to improve and refine traditional murine models of tumor growth and metastasis. Clin Exp Metastasis. 2003; 20(8):733–744. [PubMed: 14713107]
22. Klerk CP, et al. Validity of bioluminescence measurements for noninvasive in vivo imaging of tumor load in small animals. Biotechniques. 2007; 43(1 Suppl):7–13. 30. [PubMed: 17936938]
23. Contero A, et al. High-throughput quantitative bioluminescence imaging for assessing tumor burden. Methods Mol Biol. 2009; 574:37–45. [PubMed: 19685298]
24. Plunkett W, Huang P, Gandhi V. Preclinical characteristics of gemcitabine. Anticancer Drugs. 1995; 6(Suppl 6):7–13. [PubMed: 8718419]
25. Edinger M, et al. Advancing animal models of neoplasia through in vivo bioluminescence imaging. Eur J Cancer. 2002; 38(16):2128–2136. [PubMed: 12387838]
26. El Hilali N, et al. Combined noninvasive imaging and luminometric quantification of luciferase-labeled human prostate tumors and metastases. Lab Invest. 2002; 82(11):1563–1571. [PubMed: 12429816]
27. Sarraf-Yazdi S, et al. Use of in vivo bioluminescence imaging to predict hepatic tumor burden in mice. J Surg Res. 2004; 120(2):249–255. [PubMed: 15234220]

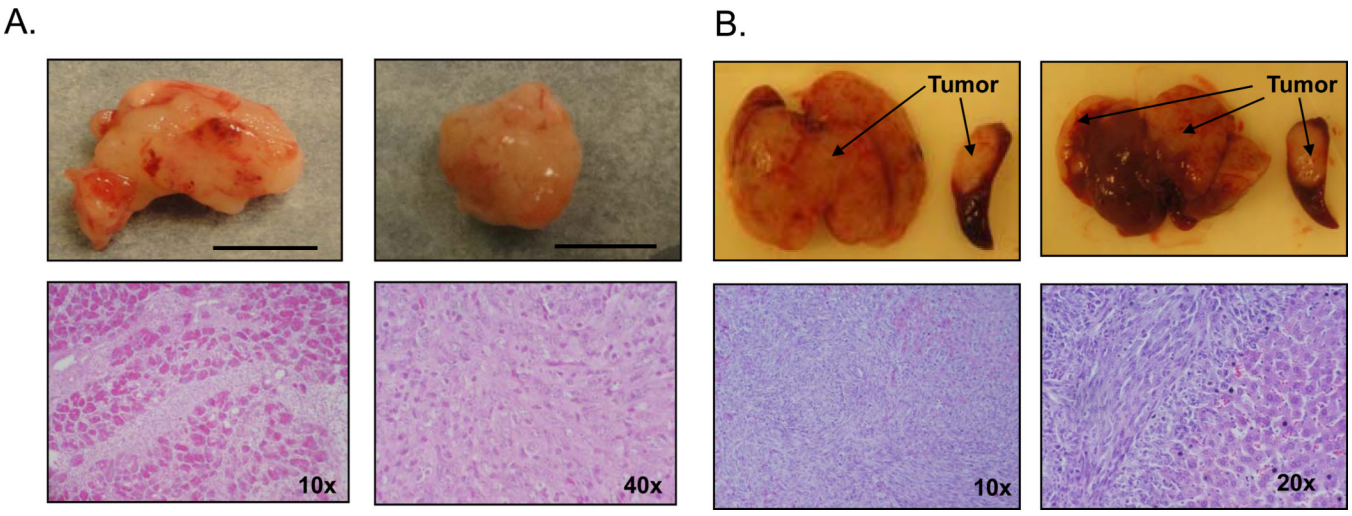

Figure 1. Pancreatic and Intrasplenic Panc02-luc injections result in consistent tumor formation

A) Representative images and H&E sections of pancreatic tumors 22 days after tumor cell injection. Scale marks 1cm. B) Representative images and H&E sections of metastatic liver tumors 15 days after intrasplenic tumor cell injection.

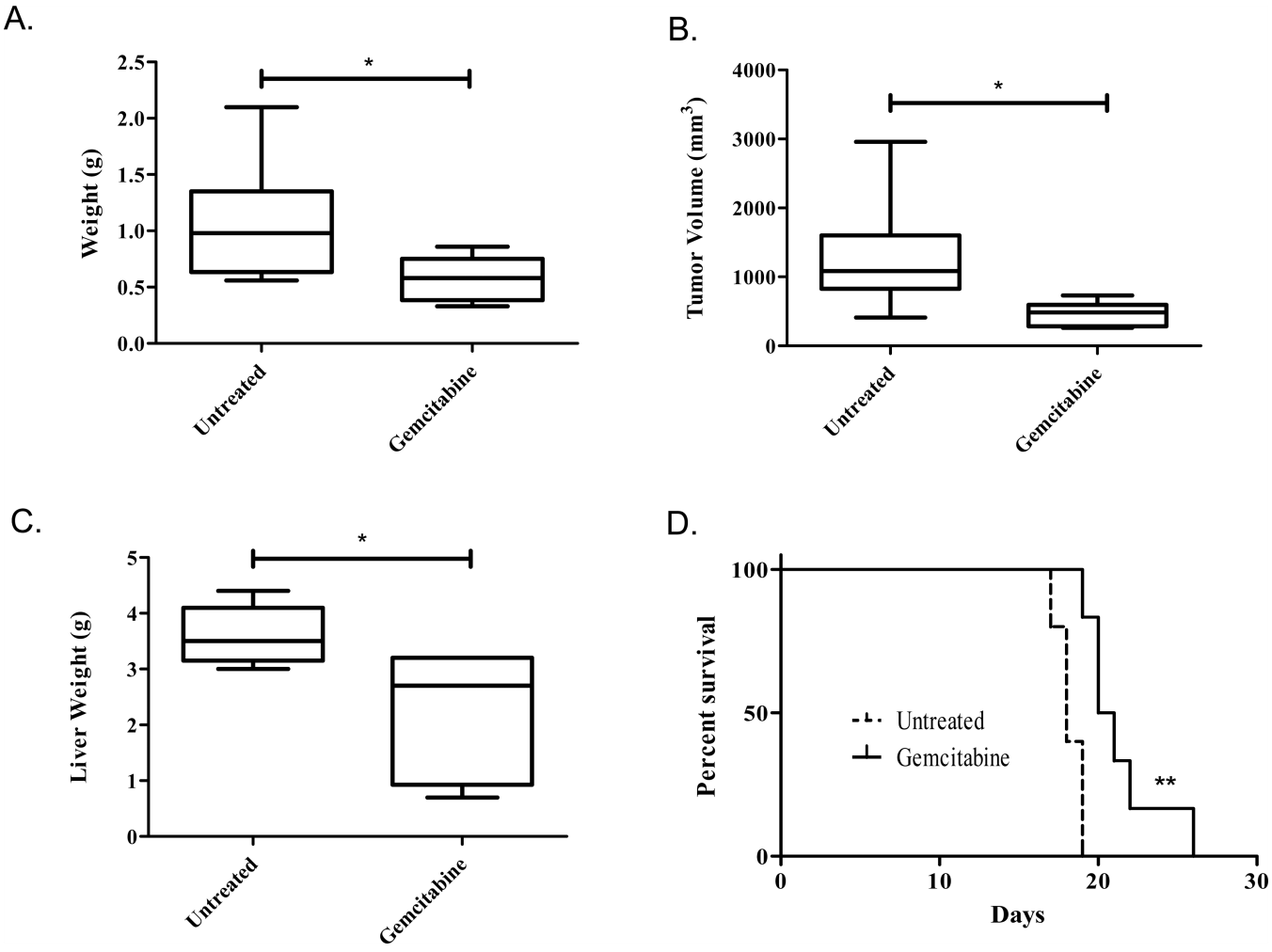

Figure 2. Gemcitibine decreases tumor burden of localized and metastatic tumors and enhances survival

Pancreatic injection (A&B): Mice either received no treatment (n=5) or an i.p. injection of 20mg/kg gemcitabine on days 7, 10, 13, 16, and 19 post-tumor cell injection (n=9). All animals were sacrificed on day 22, their tumors isolated and tumor weight (A) and volume (B) taken as a measure of tumor burden. The group means are graphed along with the SEM. *Intrasplenic Injection (C&D):* C) mice either received no treatment (n=6) or an ip injection of 20mg/kg gemcitabine on days 7, 10, and 13 post-tumor cell injection (n=6). All animals were sacrificed on day 15 and their livers weighed as a measure of tumor burden. The group means are graphed along with the SEM. D) Mice were either left untreated (n=5) or treated with 20mg/kg gemcitabine on days 7, 10, 13, and 16 (n=6). Morbundity was determined by a blind investigator and plotted with a Kaplan Meier survival curve. *P<0.05 and **P<0.005

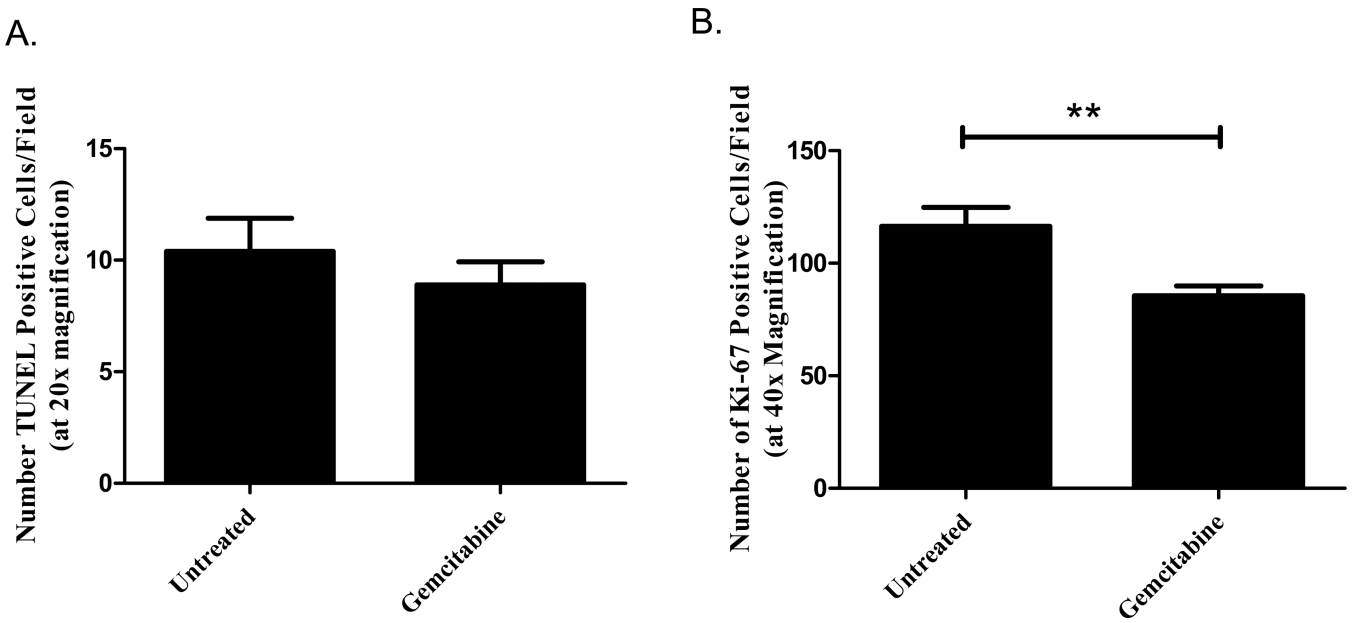

Figure 3. Gemcitabine decreases proliferation in the localized tumor model

Mice were treated with 20mg/kg gemcitabine on Days 7, 10, 13, 16, and 19 post-orthotopic Panc02 injection. Following sacrifice on Day 22, tumor sections were analyzed for apoptosis and proliferation. While gemcitabine therapy did not alter the number of TUNEL-positive cells (A, $P>0.05$), treatment did reduce the number of Ki-67 positive cells compared to the untreated group (B, $^{**}P<0.005$). The group means of at least 3 random fields per sample are graphed along with the SEM.

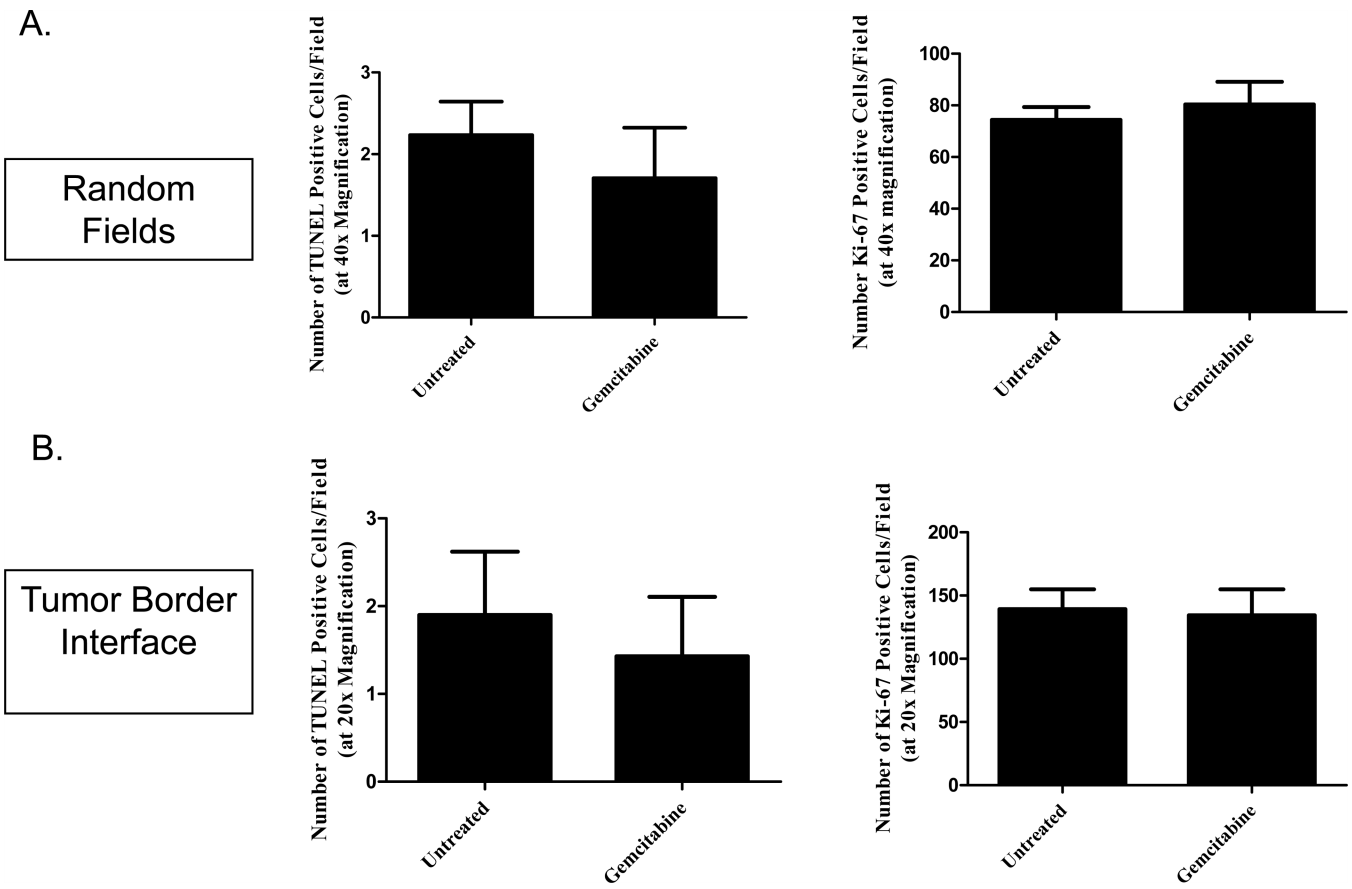

Figure 4. Gemcitabine does not affect TUNEL or Ki-67 expression in metastatic liver tumors

Mice were treated with 20mg/kg gemcitabine on Days 7, 10, and 13 post-orthotopic Panc02 injection. Following sacrifice on Day 15, tumor sections were analyzed for apoptosis and proliferation using both random fields throughout the tumor (A) and on the tumor-border interface (B). There were no significant differences between untreated and gemcitabine-treated tumors with either TUNEL (left) or Ki-67 (right) quantification ($P>0.05$). The group means of at least 3 random fields per sample are graphed along with the SEM.

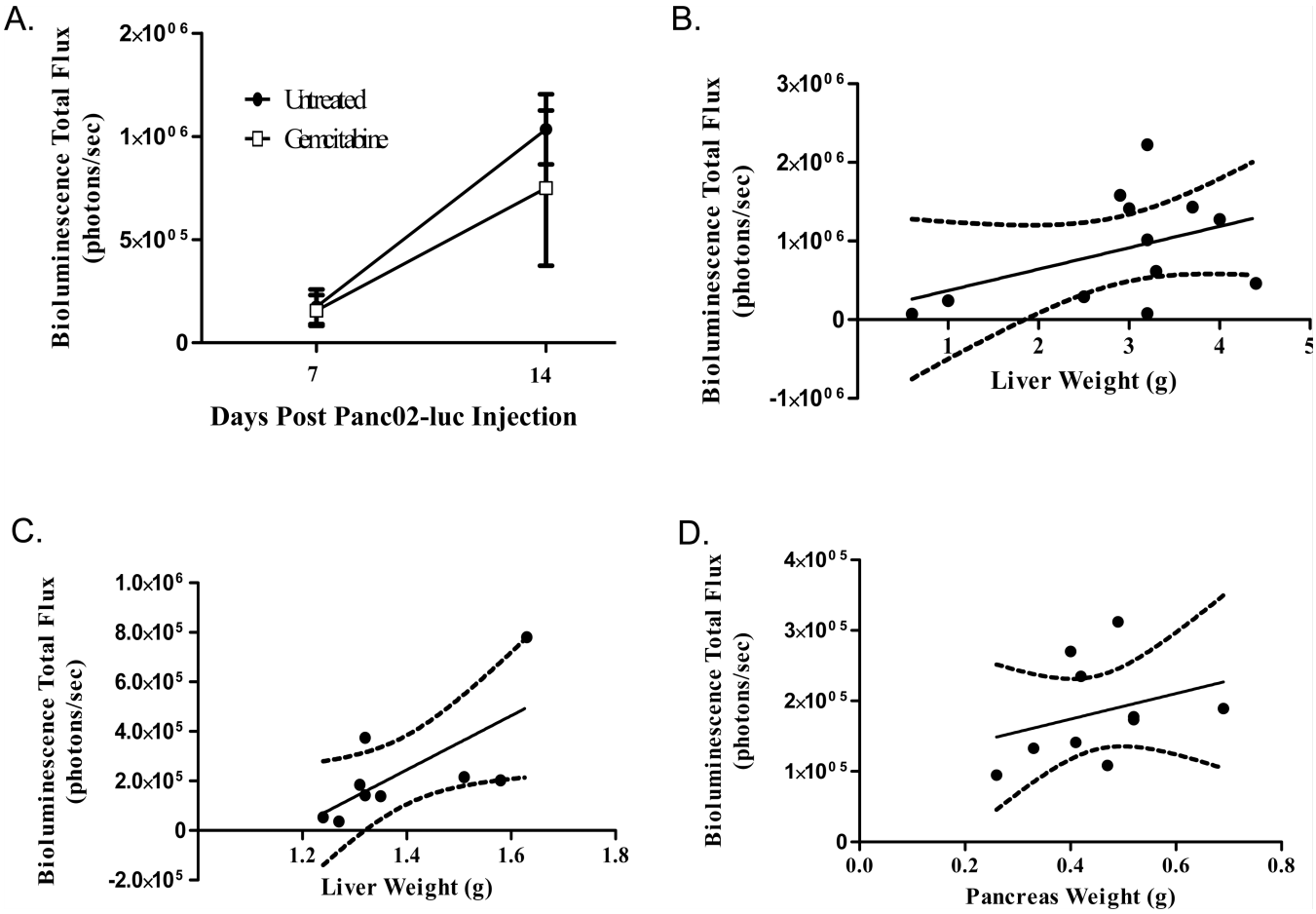

Figure 5. Bioluminescence Imaging does not accurately predict tumor burden

(A&B): Mice were received an intrasplenic injection of 1 million Panc02-luc cells and either received no treatment (n=6) or an i.p. injection of 20mg/kg gemcitabine on days 7, 10, and 13 post-tumor cell injection (n=6). On days 7 and 14, BLI was performed on all mice following an i.p. injection of 3mg D-luciferin. *A)* There were no statistically significant differences in BLI between the untreated and gemcitabine-treated groups on either day ($P>0.05$). *B)* Liver weight did not closely correlate with BLI output though linear regression showed a relationship did exist. *(C)* 1 million Panc02-luc cells were injected intrasplenically on day 0 (n=9). On day 16, mice were injected with 3mg D-luciferin and liver harvested for ex vivo BLI. Though a relationship exists ($P<0.05$), BLI output does not closely correlate with liver weight ($R^2=0.4727$). *(D)* 1 million Panc02-luc cells were injected orthotopically on day 0 (n=9). On day 15, mice were injected with 3mg D-luciferin and pancreas tumors harvested for ex vivo BLI. BLI output does not correlate with tumor weight ($P>0.05$, $R^2=0.0920$).